Cooperative spontaneous emission from indistinguishable atoms in arbitrary motional quantum states

François Damanet,[1] Daniel Braun,[2] and John Martin[1]

[1]*Institut de Physique Nucléaire, Atomique et de Spectroscopie, CESAM, Université de Liège, Bâtiment B15, B-4000 Liège, Belgium*
[2]*Institut für theoretische Physik, Universität Tübingen, 72076 Tübingen, Germany*

We investigate superradiance and subradiance of indistinguishable atoms with quantized motional states, starting with an initial total state that factorizes over the internal and external degrees of freedom of the atoms. Due to the permutational symmetry of the motional state, the cooperative spontaneous emission, governed by a recently derived master equation [F. Damanet *et al.*, Phys. Rev. A **93**, 022124 (2016)], depends only on two decay rates γ and γ_0 and a single parameter Δ_{dd} describing the dipole-dipole shifts. We solve the dynamics exactly for $N = 2$ atoms, numerically for up to 30 atoms, and obtain the large-N limit by a mean-field approach. We find that there is a critical difference $\gamma_0 - \gamma$ that depends on N beyond which superradiance is lost. We show that exact nontrivial dark states (i.e., states other than the ground state with vanishing spontaneous emission) only exist for $\gamma = \gamma_0$ and that those states (dark when $\gamma = \gamma_0$) are subradiant when $\gamma < \gamma_0$.

I. INTRODUCTION

Cooperative spontaneous emission of light from excited atoms, which results from their common coupling with the surrounding electromagnetic field, is a central field of research in quantum optics. In a seminal paper [1], Dicke showed that spontaneous emission can be strongly enhanced when atoms are close to each other in comparison to the wavelength of the emitted radiation. This phenomenon, called superradiance, and its counterpart corresponding to reduced spontaneous emission, called subradiance, were first considered for distinguishable atoms at fixed positions. Depending on the geometrical arrangement of the atoms in space, deeper analyses showed later that virtual photon exchanges between atoms were likely to destroy superradiance [2–4]. Due to the complexity involved by the exact treatment of these dipole-dipole interactions, analytical characterizations of superradiance have been found only for particular geometries or for a small number of atoms [4–9]. Yet cooperative emission processes are not restricted to small atomic samples. They can also be observed in dilute atomic systems for which the near-field contributions of the dipole-dipole interactions are insignificant. Recent studies concern single-photon superradiance [10–13], subradiance in cold atomic gases [14,15], collective Lamb shift [16,17], and localization of light [18,19]. Moreover, super- and subradiance can be explained using a quantum multipath interference approach and can be simulated from the measurement of higher-order intensity correlation functions on atoms separated by a distance larger than the emission wavelength [20,21].

The atomic motion can have a significant influence on the spontaneous emission and scattering of light [22–27] and vice versa (see, e.g., [28–34]). However, its role on cooperative emission processes is not yet fully understood, especially in large laser-driven atomic systems [35]. The interplay of atomic motion and cooperative processes has been the subject of recent experiments [36–40] and can lead to interesting effects such as supercooling of atoms [41] or superradiant Rayleigh scattering from a Bose-Einstein condensate (BEC) [42]. In hot atomic samples, the motion can be treated classically and leads to Doppler broadenings of the spectral lines. In (ultra)cold atomic samples, the quantum nature of the motion and the indistinguishability must be taken into account, as they also lead to strong modifications of the dynamics. In this paper we study super- and subradiance from indistinguishable atoms, taking into account recoil, quantum fluctuations of the atomic positions, and quantum statistics. To this end, we solve a recently derived master equation describing the cooperative spontaneous emission of light by N two-level atoms in arbitrary quantum motional states [43].

Indistinguishability of atoms profoundly changes their internal dynamics as compared to that of distinguishable atoms. For distinguishable atoms with classical positions, the solution of the master equation depends considerably on the geometrical arrangement of the atoms in space. When describing each atom as a two-level atom, the internal state of the atoms thus evolves in the full Hilbert space of dimension 2^N. The same general considerations can be made when the atomic positions are treated quantum mechanically since, despite changed rates and level shifts, the master equation [43] then retains the same global form with the same Lindblad operators. Hence, each configuration must be dealt with case by case. However, for indistinguishable atoms, the global state has to be invariant under exchange of the atoms. For initial states that are separable between the internal degrees of freedom and the motional degrees of freedom, both internal and motional states must be invariant under permutation of atoms. Furthermore, on the time scale of the spontaneous emission in the optical domain, the motional state can be considered frozen such that the permutational symmetry of the motional state prevails throughout the entire emission process. This leads to a permutationally invariant average Lindblad-Kossakowski matrix of emission rates and permutationally invariant dipole shifts, which limits the quantum dynamics also of the internal degrees of freedom to the permutation-invariant subspace of dimension $O(N^2)$ of the global Hilbert space [44,45], thus greatly simplifying the problem. However, the quantum fluctuations of the positions of the atoms modify the cooperative effect of collective emission, thus leading back from superradiance to individual

spontaneous emission for large enough quantum uncertainty in the positions.

The paper is organized as follows. In Sec. II we discuss the general form of the master equation for the atomic internal dynamics derived in [43] in the case of indistinguishable atoms. In particular, we show that the master equation preserves permutation invariance of the internal state. In Sec. III we write the master equation in the coupled spin basis as it is particularly suited for permutation-invariant states. Finally, in Sec. IV we solve the master equation analytically for $N = 2$ and numerically for up to $N = 30$ atoms in order to study the impact of the quantization of the atomic motion on super- and subradiance.

II. GENERAL FORM OF THE MASTER EQUATION FOR INDISTINGUISHABLE ATOMS

A. Symmetry of the initial state

Let us consider N indistinguishable atoms in a mixture ρ_A. Each wave function of the mixture has to be either symmetric (bosons) or antisymmetric (fermions) under exchange of atoms. Let P_π denote the permutation operator of a permutation π defined through exchange of the atomic labels. We have [see Eq. (A3)]

$$P_\pi \rho_A P_{\pi'}^\dagger = (\pm 1)^{p_\pi + p_{\pi'}} \rho_A \; \forall \pi, \pi', \tag{1}$$

where p_π is the parity of the permutation π (even or odd) and $(\pm 1)^{p_\pi}$ the phase factor picked up accordingly for bosons (upper sign) or fermions (lower sign). Moreover, the Born approximation performed in [43] assumes that the initial atomic state is separable, i.e., $\rho_A(0) = \rho_A^{\rm in}(0) \otimes \rho_A^{\rm ex}$, with $\rho_A^{\rm ex}$ the motional density operator at time $t = 0$. This implies that both internal and external states are invariant under permutation of atoms [see Eq. (A7)],

$$P_\pi^{\rm in} \rho_A^{\rm in}(0) P_\pi^{\rm in\dagger} = \rho_A^{\rm in}(0) \; \forall \pi,$$
$$P_\pi^{\rm ex} \rho_A^{\rm ex} P_\pi^{\rm ex\dagger} = \rho_A^{\rm ex} \; \forall \pi. \tag{2}$$

B. Standard form

In the interaction picture, the master equation for the reduced density matrix $\rho_A^{\rm in}(t)$ describing the internal dynamics of the system A composed of N indistinguishable atoms takes the standard form [43]

$$\frac{d\rho_A^{\rm in}(t)}{dt} = \mathcal{L}[\rho_A^{\rm in}(t)] = -\frac{i}{\hbar}[H_{\rm dd}, \rho_A^{\rm in}(t)] + \mathcal{D}[\rho_A^{\rm in}(t)], \tag{3}$$

with the Liouvillian superoperator $\mathcal{L}[\cdot]$ involving the dipole-dipole Hamiltonian

$$H_{\rm dd} = \hbar \Delta_{\rm dd} \sum_{i \neq j}^N \sigma_+^{(i)} \sigma_-^{(j)}, \tag{4}$$

with $\Delta_{\rm dd}$ the dipole-dipole shifts, and the dissipator

$$\mathcal{D}[\rho_A^{\rm in}] = \gamma \sum_{i \neq j}^N \left(\sigma_-^{(j)} \rho_A^{\rm in} \sigma_+^{(i)} - \frac{1}{2}\{\sigma_+^{(i)} \sigma_-^{(j)}, \rho_A^{\rm in}\} \right)$$
$$+ \gamma_0 \sum_{i=1}^N \left(\sigma_-^{(i)} \rho_A^{\rm in} \sigma_+^{(i)} - \frac{1}{2}\{\sigma_+^{(i)} \sigma_-^{(i)}, \rho_A^{\rm in}\} \right), \tag{5}$$

with γ_0 the single-atom spontaneous emission rate and γ the cooperative (off-diagonal) decay rates. In Eqs. (4) and (5), $\sigma_+^{(j)} = (|e\rangle\langle g|)_j$ and $\sigma_-^{(j)} = (|g\rangle\langle e|)_j$ are the ladder operators for atom j with $|g\rangle$ ($|e\rangle$) the lower (upper) atomic level of energy $-\hbar\omega_0/2$ ($\hbar\omega_0/2$). Note that in Eq. (4) we do not consider diagonal terms ($i = j$) corresponding to the Lamb shifts. They can be discarded by means of a renormalization of the atomic frequency. The fact that all off-diagonal ($i \neq j$) decay rates are equal and all dipole-dipole shifts are equal for any pairs of atoms is merely a consequence of the indistinguishability of atoms (see Appendix B for a formal derivation).

The master equation (3) is valid for arbitrary motional quantum states and can be applied well-beyond the Lamb-Dicke regime. All effects related to the quantization of the atomic motion are encoded in the values taken by the dipole-dipole shift $\Delta_{\rm dd}$ and the decay rate γ. We give their exact expressions for arbitrary motional symmetric or antisymmetric states in Appendix B [see Eqs. (B12) and (B13)]. They depend not only on the average atomic positions (classical atomic positions) but also on their quantum fluctuations and correlations as described by the quantum motional (external) state $\rho_A^{\rm ex}$ of the atoms. In particular, their values can strongly depend on the statistical nature (bosonic or fermionic) of the atoms. In the next section, we give analytical expressions of γ for BECs in different regimes.

C. Off-diagonal decay rates γ for Bose-Einstein condensates

We first consider the case of a noninteracting BEC confined in an isotropic harmonic trap at zero temperature. In this case, all atoms are in the same motional state $\phi(\mathbf{r}) = e^{-|\mathbf{r}|^2/4\ell^2}/(\sqrt{2\pi}\ell)^{3/2}$, with $\ell = \sqrt{\hbar/2M\Omega}$ the width of the spatial density, M the atomic mass, and Ω the trap frequency. The decay rate γ for this motional state follows from Eq. (B15) with $\rho_1(\mathbf{r}) = |\phi(\mathbf{r})|^2$ and is given by

$$\gamma = \gamma_0 e^{-\eta^2}, \tag{6}$$

with $\eta = k_0\ell$ the Lamb-Dicke parameter and k_0 the radiation wave number. Since the size of a BEC typically lies in the range 10–10^3 μm [46], significant modifications of the decay rate γ should be observable for internal transitions in the visible and near-infrared domain.

We now consider the case of a BEC with strong repulsive interactions at zero temperature, for which the spatial density $\rho_1(\mathbf{r})$ is given in the Thomas-Fermi approximation by

$$\rho_1(\mathbf{r}) = \begin{cases} \frac{M}{4\pi\hbar^2 a}[\mu - V_{\rm ext}(\mathbf{r})] & \text{for } \mu \geqslant V_{\rm ext}(\mathbf{r}) \\ 0 & \text{for } \mu < V_{\rm ext}(\mathbf{r}), \end{cases} \tag{7}$$

where a is the scattering length, μ is the chemical potential, and $V_{\rm ext}(\mathbf{r}) = M\Omega^2 r^2/2$ is the harmonic trap potential. Inserting Eq. (7) into Eq. (B15) yields after integration

$$\gamma = 225\gamma_0 \frac{[3x\cos x + (x^2 - 3)\sin x]^2}{x^{10}}, \tag{8}$$

where $x = \eta\sqrt[5]{60Na/\ell}$, with N the number of atoms in the BEC. Figure 1 shows Eq. (8) as a function of x. In particular, when $x \to 0$ (small recoil), γ tends to γ_0.
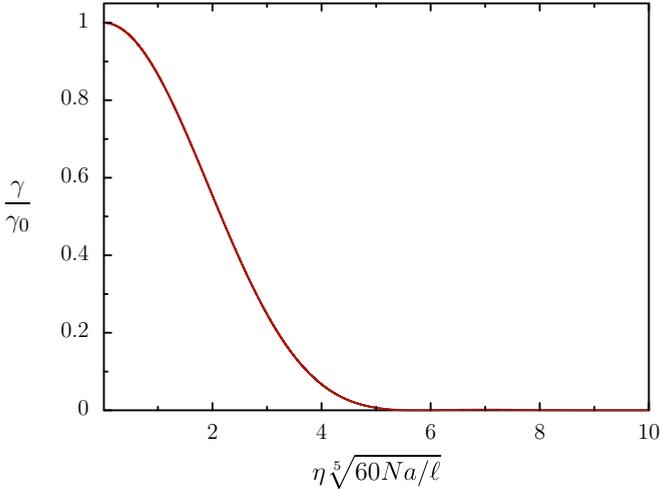
FIG. 1. Off-diagonal decay rate γ as a function of the dimensionless variable $x = \eta \sqrt[5]{60Na/\ell}$ for a BEC with strong repulsive interactions in the Thomas-Fermi limit.

We finally study the transition from a thermal cloud to a noninteracting BEC by considering a gas of trapped bosonic atoms in thermal equilibrium at finite temperature T. The spatial density of the gas is given by [47]

$$\rho_1(\mathbf{r}) = \frac{1}{N(2\pi \ell^2)^{\frac{3}{2}}} \sum_{k=1}^{\infty} \frac{z^k}{\left(1 - e^{-2k\beta\hbar\Omega}\right)^{\frac{3}{2}}} e^{-\frac{r^2}{2\ell^2}\tanh\left(\frac{k\beta\hbar\Omega}{2}\right)}, \quad (9)$$

where $z = e^{\beta\mu}$ is the fugacity and $\beta = 1/k_B T$, with k_B the Boltzmann constant. Inserting Eq. (9) into Eq. (B15) yields after integration

$$\gamma = \frac{\gamma_0}{N^2} \left[\sum_{k=1}^{\infty} \frac{z^k e^{3k\beta\hbar\Omega}}{(1 - e^{k\beta\hbar\Omega})^3} e^{-\frac{\eta^2}{2}\coth\left(\frac{k\beta\hbar\Omega}{2}\right)} \right]^2. \quad (10)$$

For $z \to 0$, Eq. (9) tends to a thermal cloud profile $\rho_1(\mathbf{r}) = e^{-(r/2R)^2}/(2\pi R^2)^{3/2}$ with $R = \sqrt{k_B T/m\Omega^2}$ and we get

$$\gamma = \gamma_0 e^{-k_0^2 R^2}, \quad (11)$$

where $e^{-k_0^2 R^2}$ is the Debye-Waller factor. Figure 2 shows Eq. (10) as a function of η for $\beta\hbar\Omega = 1/10$ and different values of the fugacity. The curves $\gamma(\eta)$ switch gradually from Eq. (11) for $z = 0$ to Eq. (6) for $z = 1$ as the fugacity is increased, as a consequence of the formation of a condensed phase (see the inset of Fig. 2). For fixed Lamb-Dicke parameter and $\beta\hbar\Omega$, γ increases monotonically with the fugacity. Hence, cooperative effects will be more pronounced when all atoms are in the condensed phase (a pure BEC).

D. Lindblad form

Before we discuss the Lindblad form of the master equation (3), let us note that the dipole-dipole Hamiltonian (4) can be rewritten in terms of collective spin operators only as

$$H_{\rm dd} = \hbar\Delta_{\rm dd}\left[J_+ J_- - \tfrac{1}{2}(N\mathbb{1} + 2J_z) \right], \quad (12)$$

where $\mathbb{1}$ is the identity operator acting on the internal atomic states, $J_\pm = \sum_{j=1}^{N} \sigma_\pm^{(j)}$ are the collective spin ladder operators,
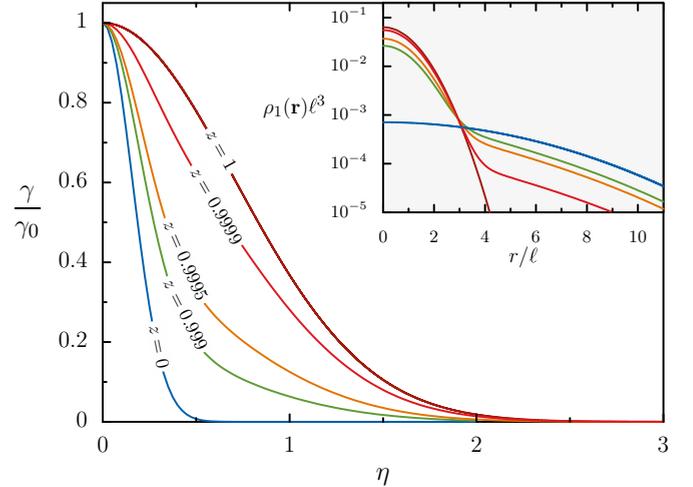

FIG. 2. Off-diagonal decay rate γ as a function of the Lamb-Dicke parameter η for a gas of trapped bosonic atoms at thermal equilibrium for $\beta\hbar\Omega = 1/10$ and different values of the fugacity, from $z = 0$ (left) to $z = 1$ (right). The inset shows spatial density profiles for the same parameters.

and $J_z = \frac{1}{2}\sum_{j=1}^{N} \sigma_z^{(j)}$ with $\sigma_z^{(j)} = (|e\rangle\langle e| - |g\rangle\langle g|)_j$. As for the dissipator (5), it also involves individual spin operators and can be rewritten as

$$\mathcal{D}[\rho_A^{\rm in}] = \gamma \left(J_- \rho_A^{\rm in} J_+ - \frac{1}{2}\{J_+ J_-, \rho_A^{\rm in}\} \right)$$
$$+ (\gamma_0 - \gamma)\left(\sum_{i=1}^{N} \sigma_-^{(i)} \rho_A^{\rm in} \sigma_+^{(i)} - \frac{1}{4}\{N\mathbb{1} + 2J_z, \rho_A^{\rm in}\} \right). \quad (13)$$

The Lindblad form is obtained from the diagonalization of the $N \times N$ matrix of decay rates

$$\boldsymbol{\gamma} = \begin{pmatrix} \gamma_0 & \gamma & \cdots & \gamma \\ \gamma & \gamma_0 & \cdots & \gamma \\ \vdots & \vdots & \ddots & \vdots \\ \gamma & \gamma & \cdots & \gamma_0 \end{pmatrix}, \quad (14)$$

with $|\gamma| \leqslant \gamma_0$ [43]. Associated with each eigenvector with nonzero eigenvalue Γ_ℓ is a Lindblad operator F_ℓ. Degenerate eigenvalues give rise to several Lindblad operators. The matrix (14) has eigenvalues

$$\Gamma_1 = \gamma_0 + (N-1)\gamma \equiv N\gamma + \Delta\gamma, \quad (15a)$$

$$\Gamma_2 = \gamma_0 - \gamma \equiv \Delta\gamma, \quad (15b)$$

with onefold and $(N-1)$-fold degeneracy, respectively. For the dynamics to be Markovian, the matrix $\boldsymbol{\gamma}$ has to be positive. This implies that $-\gamma_0/(N-1) \leqslant \gamma \leqslant \gamma_0$ and $0 \leqslant \Delta\gamma \leqslant \gamma_0 N/(N-1)$. An eigenvector $\mathbf{v}_1$ with the largest eigenvalue Γ_1 is the vector with all components equal to $1/\sqrt{N}$. The corresponding Lindblad operator is $F_1 = J_-/\sqrt{N}$. The remaining eigenvectors with degenerate eigenvalue $\Delta\gamma$ span the subspace $\mathbb{C}^{N-1}$ orthogonal to $\mathbf{v}_1$ and lead to Lindblad

operators F_ℓ. The Lindblad form of the dissipator thus reads

$$\mathcal{D}[\rho_A^{\text{in}}] = \frac{\Gamma_1}{N}\left(J_-\rho_A^{\text{in}}J_+ - \frac{1}{2}\{J_+J_-,\rho_A^{\text{in}}\}\right)$$
$$+ \Delta\gamma\left(\sum_{\ell=2}^{N} F_\ell\rho_A^{\text{in}}F_\ell^\dagger - \frac{1}{2}\{F_\ell^\dagger F_\ell,\rho_A^{\text{in}}\}\right). \quad (16)$$

When $\Delta\gamma = 0$ ($\gamma = \gamma_0$), the system evolves under the sole action of the collective spin operator J_-. As a consequence, starting from an internal symmetric state, the dynamics is restricted to the symmetric subspace of dimension $N + 1$. This is the superradiant regime [4].

When $\Delta\gamma > 0$ ($\gamma < \gamma_0$), all the additional Lindblad operators are involved in the dynamics. The superoperator multiplying $\Delta\gamma$ in Eq. (16) can be rewritten as

$$\sum_{i=1}^{N} \sigma_-^{(i)}\rho_A^{\text{in}}\sigma_+^{(i)} - \frac{J_-\rho_A^{\text{in}}J_+}{N} - \frac{1}{2}\left\{\frac{N\mathbb{1}}{2} + J_z - \frac{J_+J_-}{N},\rho_A^{\text{in}}\right\}. \quad (17)$$

Hence, it cannot be expressed as a function of collective spin operators only. However, it affects each atom identically. Therefore, the Liouvillian superoperator does not distinguish between atoms and commutes with P_π for all permutations π, i.e.,

$$P_\pi\mathcal{L}[\rho]P_\pi^\dagger = \mathcal{L}[P_\pi\rho P_\pi^\dagger]\,\forall\rho,\pi. \quad (18)$$

It couples symmetric states with the broader class of permutation-invariant states. These states, denoted hereafter by ρ_{PI}, are states satisfying [48]

$$\rho_{\text{PI}} = P_\pi\rho_{\text{PI}}P_\pi^\dagger\,\forall\pi. \quad (19)$$

They act on a subspace whose dimension grows only as N^2 [44,45].

III. MASTER EQUATION IN THE COUPLED SPIN BASIS

From now on, we will denote the internal density matrix ρ_A^{in} by ρ. In this section we express the master equation (3) in the coupled spin basis, which is particularly suited for the study of permutation-invariant states.

A. Coupled spin basis

The Hilbert space $\mathcal{H}$ of an ensemble of N two-level systems admits the Wedderburn decomposition [48–51]

$$\mathcal{H} = (\mathbb{C}^2)^{\otimes N} \simeq \bigoplus_{J=J_{\text{min}}}^{N/2} \mathcal{H}_J \otimes \mathcal{K}_J, \quad (20)$$

with $J_{\text{min}} = 0$ for even N and $1/2$ for odd N. In Eq. (20), $\mathcal{H}_J$ is the representation space of dimension $2J + 1$ on which the irreducible representations of the group SU(2) act. The number of degenerate irreducible representations with total angular momentum J is equal to the dimension

$$d_N^J = \frac{(2J + 1)N!}{(N/2 - J)!(N/2 + J + 1)!} \quad (21)$$

of the multiplicity space $\mathcal{K}_J$ on which the irreducible representations of the symmetric group S_N act. The total Hilbert
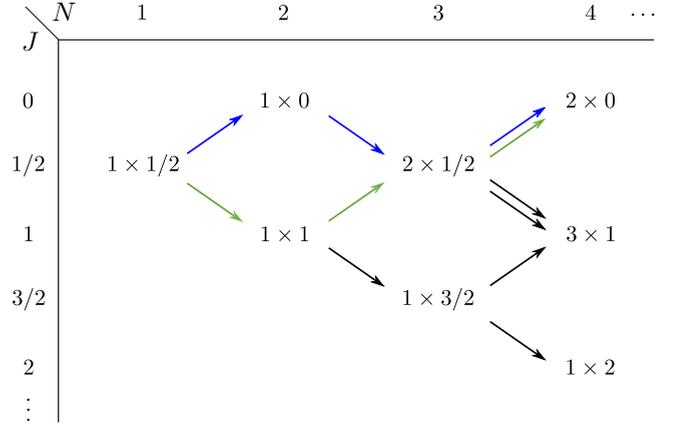

FIG. 3. Bratteli diagram representing the degeneracy structure $d_n^J \times J$ of N coupled spins $1/2$. The two colored paths leading to the same angular momentum $J = 0$ correspond to two different values of the quantum number $k_{J=0}$.

space $\mathcal{H}$ is therefore spanned by the states $|J,M,k_J\rangle \equiv |J,M\rangle \otimes |k_J\rangle$, where $|J,M\rangle$ are basis states of the subspaces $\mathcal{H}_J$ ($J = J_{\text{min}},\dots,N/2; M = -J,\dots,J$) and $|k_J\rangle$ are basis states of the subspaces $\mathcal{K}_J$ ($k_J = 1,\dots,d_N^J$). The 2^N basis states $\{|J,M,k_J\rangle\}$ form the coupled spin basis [45]. By construction, $|J,M,k_J\rangle$ are spin-J states satisfying

$$\mathbf{J}^2|J,M,k_J\rangle = J(J + 1)|J,M,k_J\rangle,$$
$$J_z|J,M,k_J\rangle = M|J,M,k_J\rangle, \quad (22)$$
$$J_\pm|J,M,k_J\rangle = \sqrt{(J \mp M)(J \pm M + 1)}|J,M \pm 1,k_J\rangle,$$

with $\mathbf{J}^2 = J_x^2 + J_y^2 + J_z^2$ and $J_m = \frac{1}{2}\sum_{j=1}^{N}\sigma_m^{(j)}$ ($m = x,y,z$). The degenerate structure of the decomposition (20) is depicted in the Bratteli diagram shown in Fig. 3. There are d_N^J ways to obtain an angular momentum J from the coupling of N spins $1/2$, each way being associated with a path in the Bratteli diagram. The quantum number $k_J = 1,\dots,d_N^J$ enables one to distinguish these different paths.

B. Permutation-invariant states in the coupled spin basis

According to the Schur-Weyl duality [52,53], any permutation P_π acts only on the multiplicity subspaces $\mathcal{K}_J$ [see decomposition (20)] and thus has the form

$$P_\pi = \bigoplus_{J=J_{\text{min}}}^{N/2} \mathbb{1}_{\mathcal{H}_J} \otimes P_J(\pi), \quad (23)$$

where $\mathbb{1}_{\mathcal{H}_J}$ is the identity operator on $\mathcal{H}_J$ and $P_J(\pi)$ is an irreducible representation of S_N of dimension d_N^J. A permutation-invariant mixed state ρ_{PI} commutes with P_π for any permutation π [see Eq. (19)] and thus admits in the coupled spin basis a block-diagonal form [48]

$$\rho_{\text{PI}} = \bigoplus_{J=J_{\text{min}}}^{N/2} \rho_J \otimes \mathbb{1}_{\mathcal{K}_J}, \quad (24)$$

where $\mathbb{1}_{\mathcal{K}_J}$ is the identity operator on $\mathcal{K}_J$ and

$$\rho_J = \sum_{M,M'=-J}^{J} \rho_J^{M,M'} |J,M\rangle\langle J,M'|, \qquad (25)$$

with the density matrix elements

$$\rho_J^{M,M'} \equiv \langle J,M,k_J|\rho_{\text{PI}}|J,M',k_J\rangle \ \forall k_J. \qquad (26)$$

The block-diagonal form illustrated in Fig. 4 shows that ρ_{PI} does not contain any coherences between blocks of different angular momenta J. For each J, there are d_N^J identical subblocks. Since the matrix elements in these blocks do not depend on the label $k_J = 1, \ldots, d_N^J$, the number of real parameters needed to specify a permutation-invariant state ρ_{PI} corresponds to the sum of the density matrix elements of all ρ_J,

$$\sum_{J=J_{\min}}^{N/2} (2J+1)^2 = \frac{1}{6}(N+1)(N+2)(N+3) = O(N^3). \quad (27)$$

This number is much smaller than the total number $(2^{2N} - 1)$ of a general N-atom density operator and highlights the convenience of this representation.

Note that a symmetric mixed state ρ_S is just a particular case of permutation-invariant state (24) with $\rho_J^{M,M'} = 0$ for $J \neq N/2$. The nonvanishing matrix elements of symmetric states all lie in the upper block $\rho_{N/2}$ of dimension $N+1$ depicted in Fig. 4.
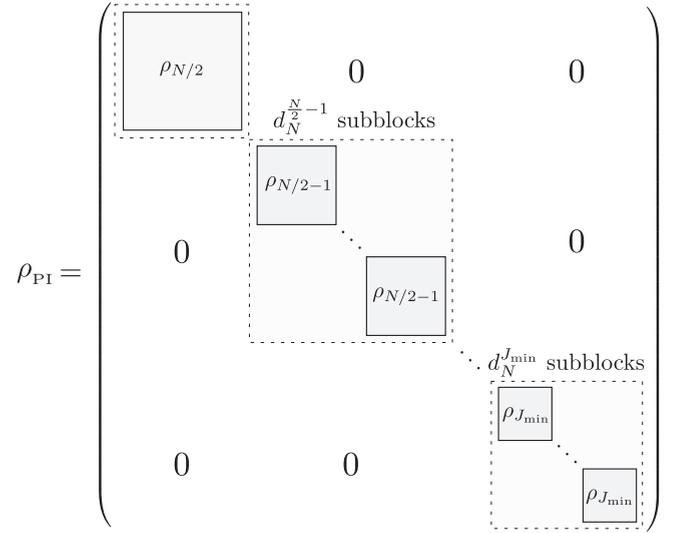

FIG. 4. Block-diagonal form of the density matrix representing a permutation-invariant state in the coupled spin basis. To each value of the angular momentum J corresponds d_N^J subblocks of dimension $(2J+1) \times (2J+1)$. The block with $J = N/2$ is unique and is spanned by symmetric states.

C. Projection of the master equation in the coupled spin basis

Let us write the master equation (3) in terms of matrix elements of the density operator in the coupled spin basis. By inserting Eq. (24) into Eq. (3) and using Eqs. (12) and (22), we get

$$[H_{\text{dd}},\rho(t)] = \hbar\Delta_{\text{dd}} \sum_{J=J_{\min}}^{N/2} \sum_{M,M'=-J}^{J} \rho_J^{M,M'}(t)(M'^2 - M^2)|J,M\rangle\langle J,M'| \otimes \mathbb{1}_{\mathcal{K}_J}, \qquad (28)$$

$$\mathcal{D}[\rho(t)] = \sum_{J=J_{\min}}^{N/2} \sum_{M,M'=-J}^{J} \rho_J^{M,M'}(t) \left\{ \gamma A_-^{J,M} A_-^{J,M'} |J,M-1\rangle\langle J,M'-1| \otimes \mathbb{1}_{\mathcal{K}_J} - \frac{1}{2}[\gamma(A_-^{J,M})^2 + \gamma(A_-^{J,M'})^2 \right.$$

$$\left. + \Delta\gamma(N+M+M')]|J,M\rangle\langle J,M'| \otimes \mathbb{1}_{\mathcal{K}_J} + \Delta\gamma \sum_{j=1}^{N} \sigma_-^{(j)}[|J,M\rangle\langle J,M'| \otimes \mathbb{1}_{\mathcal{K}_J}]\sigma_+^{(j)} \right\}. \qquad (29)$$

The last term in Eq. (29) cannot be written solely in terms of collective spin operators but affects each atom identically. It has been evaluated in [44] and reads

$$\sum_{j=1}^{N} \sigma_-^{(j)}[|J,M\rangle\langle J,M'| \otimes \mathbb{1}_{\mathcal{K}_J}]\sigma_+^{(j)}$$

$$= \frac{1}{2J} A_-^{J,M} A_-^{J,M'} \left(1 + \frac{\alpha_N^{J+1}(2J+1)}{d_N^J(J+1)}\right)|J,M-1\rangle\langle J,M'-1| \otimes \mathbb{1}_{\mathcal{K}_J} + \frac{B_-^{J,M} B_-^{J,M'}\alpha_N^J}{2Jd_N^{J-1}}|J-1,M-1\rangle\langle J-1,M'-1| \otimes \mathbb{1}_{\mathcal{K}_{J-1}}$$

$$+ \frac{D_-^{J,M} D_-^{J,M'}\alpha_N^{J+1}}{2(J+1)d_N^{J+1}}|J+1,M-1\rangle\langle J+1,M'-1| \otimes \mathbb{1}_{\mathcal{K}_{J+1}}, \qquad (30)$$

where

$$A_\pm^{J,M} = \sqrt{(J \mp M)(J \pm M + 1)}, \qquad (31)$$

$$B_-^{J,M} = -\sqrt{(J+M)(J+M-1)}, \qquad (32)$$

$$D_-^{J,M} = \sqrt{(J-M+1)(J-M+2)}, \qquad (33)$$

and

$$\alpha_N^J = \sum_{J'=J}^{N/2} d_N^{J'}. \tag{34}$$

Equation (28) shows that dipole-dipole interactions do not couple blocks of different angular momentum J, but couple nondiagonal ($M \neq M'$) density matrix elements within a block. The term (30) describes transitions giving rise to energy loss due to photon emissions, since it reduces the value of the quantum numbers M and M' by one unit. Such transitions from a block of angular momentum J occur either within a same block or in neighboring blocks of angular momentum $J \pm 1$. The former preserve the symmetry of the state while the latter modify it.

By injecting Eqs. (28) and (29) into the master equation (3) and projecting onto the states $|J,M,k_J\rangle$, we get a system of $O(N^3)$ [see Eq. (27)] differential equations for the density matrix elements $\rho_J^{MM'}(t)$ that reads

$$\begin{aligned}
\frac{d\rho_J^{M,M'}(t)}{dt} &= -\Gamma^{(1)}_{\substack{M,M'\\J}} \rho_J^{M,M'}(t) + \Gamma^{(2)}_{\substack{M+1,M'+1\\J}} \rho_J^{M+1,M'+1}(t) \\
&\quad + \Gamma^{(3)}_{\substack{M+1,M'+1\\J+1}} \rho_{J+1}^{M+1,M'+1}(t) \\
&\quad + \Gamma^{(4)}_{\substack{M+1,M'+1\\J-1}} \rho_{J-1}^{M+1,M'+1}(t),
\end{aligned} \tag{35}$$

with

$$\begin{aligned}
\Gamma^{(1)}_{\substack{M,M'\\J}} &= i\Delta_{dd}(M'^2 - M^2) + \frac{\gamma}{2}[(A_-^{J,M})^2 + (A_-^{J,M'})^2] \\
&\quad + \frac{\Delta\gamma}{2}(N + M + M'),
\end{aligned}$$

$$\Gamma^{(2)}_{\substack{M+1,M'+1\\J}} = A_+^{J,M} A_+^{J,M'} \left[\gamma + \frac{\Delta\gamma}{2J}\left(1 + \frac{\alpha_N^{J+1}(2J+1)}{d_N^J(J+1)}\right)\right],$$

$$\Gamma^{(3)}_{\substack{M+1,M'+1\\J+1}} = \Delta\gamma \frac{B_-^{J+1,M+1} B_-^{J+1,M'+1} \alpha_N^{J+1}}{2(J+1)d_N^J},$$

$$\Gamma^{(4)}_{\substack{M+1,M'+1\\J-1}} = \Delta\gamma \frac{D_-^{J-1,M+1} D_-^{J-1,M'+1} \alpha_N^J}{2J d_N^J}. \tag{36}$$

Equations (36) for the transition rates show that the populations $\rho_J^{M,M}$ are decoupled from the coherences $\rho_J^{M,M'}$ ($M \neq M'$). More specifically, coherences specified by M,M' are only coupled to coherences with the same difference $M - M'$, and populations $\rho_J^{M,M}$ can only feed populations $\rho_{J'}^{M',M'}$ with $M' \leqslant M$ and $J' \geqslant (J - M)/2$. This can be seen from Eqs. (35) and (36) and Fig. 5, which shows the couplings between the populations together with the corresponding rates. Indeed, in Eq. (35), the derivative of $\rho_{J'}^{M',M'}$ depends only on density matrix elements with equal or larger quantum numbers M, which implies that starting from a state with a given M, only states with $M' \leqslant M$ can be populated during the dynamics. As for the quantum number J', it can decrease or increase through the channels with rates $\Gamma^{(3)}$ and $\Gamma^{(4)}$ (see Fig. 5). However, it cannot decrease indefinitely. Consider the initial state $|J,M\rangle$: All states $|J - Q, M - Q\rangle$ with positive half-integer Q can be populated provided $J - Q \geqslant J_{\min}$ and $J - Q \geqslant M - Q \geqslant -(J - Q)$. The first inequality of the latter expression is always satisfied since $M \leqslant J$, but the
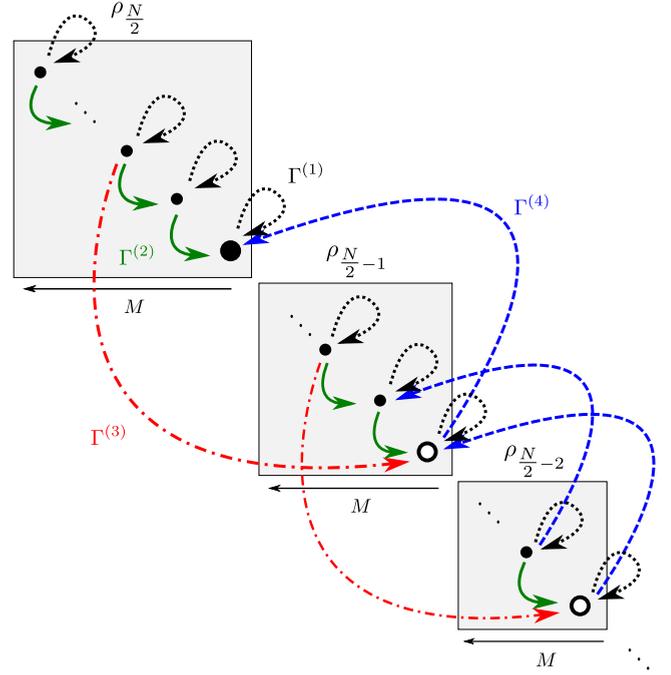

FIG. 5. Couplings between the populations $\rho_J^{M,M}$ (small closed circles) lying in the different blocks ρ_J of angular momentum $J = N/2, N/2 - 1, N/2 - 2, \dots$ (gray squares), as described by Eq. (35). The large closed and open circles at the bottom right of each block are the populations $\rho_J^{-J,-J}$ corresponding to subradiant states when $\Delta\gamma = 0$ (see Sec. IV B). The arrows show the different couplings between populations characterized by the rates $\Gamma^{(r)}$ (with $r = 1,2,3,4$ and where the subscripts have been dropped for the sake of clarity). The rates $\Gamma^{(1)}$ and $\Gamma^{(2)}$ are related to transitions within a block, while the rates $\Gamma^{(3)}$ and $\Gamma^{(4)}$ (proportional to $\Delta\gamma$) are related to transitions between different blocks ρ_J. This diagram shows that starting with the initial condition $\rho_J^{M,M}(0) = 1$, only populations $\rho_{J'}^{M',M'}$ with $M' \leqslant M$ and $J' \geqslant (J - M)/2$ can be nonzero during the radiative decay. When $\Delta\gamma > 0$, $\Gamma^{(3)}$ and $\Gamma^{(4)}$ are nonzero and the state $|N/2, -N/2\rangle$ (large closed circle) is the only stationary state for any initial conditions.

second inequality imposes $Q \leqslant (J + M)/2$. This in turn implies the minimal value $(J - M)/2$ for the quantum number $J' \equiv J - Q$.

IV. SOLUTIONS OF THE MASTER EQUATION

The solutions of the master equation for indistinguishable atoms only involve the rates γ, $\Delta\gamma = \gamma_0 - \gamma$, and Δ_{dd}. In this section we compute numerical solutions up to 30 atoms for different values of these rates. The solutions allow us to study the modifications of super- and subradiance arising from a proper quantum treatment of the atomic motion. In addition, we obtain analytical results for large N by applying a mean-field approximation.

In order to quantify the modifications in the release of energy from the atomic system, we calculate the normalized radiated energy rate [4]

$$I(t) = -\frac{d}{dt}\langle J_z\rangle(t). \tag{37}$$

For permutation-invariant states (24), Eq. (37) can be expressed in terms of the populations $\rho_J^{M,M}$ as

$$I(t) = -\sum_{J=J_{\min}}^{N/2} d_N^J \sum_{M=-J}^{J} M \frac{d\rho_J^{M,M}(t)}{dt}. \quad (38)$$

By inserting Eq. (35) into (38) and after algebraic manipulations, we get

$$I(t) = \sum_{J=J_{\min}}^{N/2} d_N^J \sum_{M=-J}^{J} c_J^M \rho_J^{M,M}(t) \quad (39)$$

with positive coefficients c_J^M given by

$$c_J^M = (J + M)(J - M + 1)\gamma + \left(M + \frac{N}{2}\right)\Delta\gamma. \quad (40)$$

A. Superradiance

The superradiance phenomenon is usually observed when the atoms are initially in a symmetric internal state $|N/2, M\rangle$. In this section we choose for initial state the symmetric state $|N/2, N/2\rangle \equiv |e, e, \ldots, e\rangle$. This choice allows us to study the superradiant radiative cascade starting from the highest energy level.

1. Analytical results for two atoms

For two atoms, a simple analytical solution of the master equation can be obtained and is given in Appendix C. For the initial condition $\rho(0) = |1, 1\rangle\langle 1, 1| \equiv |e, e\rangle\langle e, e|$, the radiated energy rate (39) resulting from the solution (C3) given in the Appendix reads

$$I(t) = \frac{e^{-2(\gamma + \Delta\gamma)t}}{(2\gamma + \Delta\gamma)\Delta\gamma}[(2\gamma + \Delta\gamma)^2\Delta\gamma + \Delta\gamma^2(2\gamma + \Delta\gamma)$$
$$+ (2\gamma + \Delta\gamma)^3(e^{\Delta\gamma t} - 1) + \Delta\gamma^3(e^{(2\gamma + \Delta\gamma)t} - 1)]. \quad (41)$$

In the absence of quantum fluctuations of the atomic positions and for colocated atoms [43], i.e., when $\Delta\gamma = 0$ ($\gamma = \gamma_0$), pure superradiance occurs during which all symmetric Dicke states $|1, 1\rangle$, $|1, 0\rangle$, and $|1, -1\rangle$ are gradually populated. In this case, Eq. (41) reduces to the superradiant radiated energy rate

$$I(t) = 2\gamma_0 e^{-2\gamma_0 t}(1 + 2\gamma_0 t). \quad (42)$$

When $\Delta\gamma > 0$, the singlet state $|0, 0\rangle$ is coupled to the symmetric Dicke states and the radiated energy rate is reduced at small times, as can be seen in Fig. 6. When $\gamma = 0$, $\Delta\gamma = \gamma_0$ and Eq. (41) reduces to the pure exponential decay characteristic of individual spontaneous emission

$$I(t) = 2\gamma_0 e^{-\gamma_0 t}. \quad (43)$$

2. Numerical results for N > 2

In this section we solve numerically the set of coupled equations (35) for the initial condition $\rho(0) = \rho_{N/2}^{N/2, N/2} = |e, e, \ldots, e\rangle\langle e, e, \ldots, e|$ and for different values of $\Delta\gamma$. We then compute the radiated energy rate (39). Figure 7 shows $I(t)$, as a function of time, from 3 to 30 atoms, where each panel corresponds to a different value of $\Delta\gamma$. For $\Delta\gamma = 0$, pure superradiance occurs (first panel). For $\Delta\gamma = \gamma_0$, the
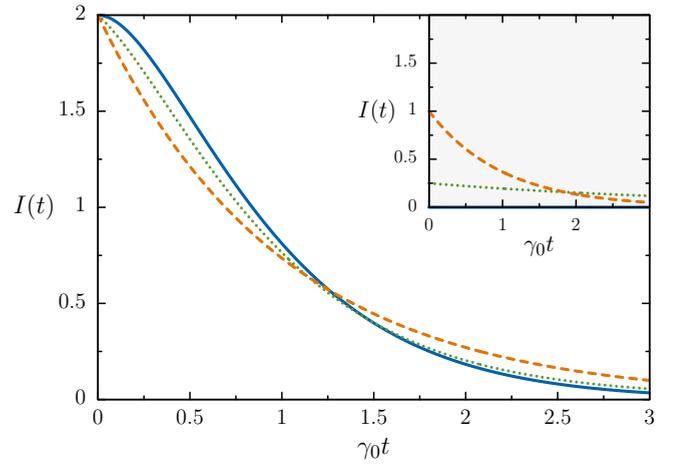

FIG. 6. Radiated energy rate for two atoms in the initial state $|e, e\rangle$ as a function of time for $\gamma = \gamma_0$ (blue solid curve), $\gamma = 3\gamma_0/4$ (green dotted curve), and $\gamma = 0$ (orange dashed curve). The blue solid curve corresponds to pure superradiance [Eq. (42)], the orange dashed curve to independent spontaneous emission [Eq. (43)], and the green dotted curve to altered superradiance [Eq. (41)]. The inset shows the radiated energy rate for the initial state $|0, 0\rangle$ and the same parameters.

radiated energy rate decreases according to $I(t) = N\gamma_0 e^{-\gamma_0 t}$, as is typical of individual spontaneous emission (last panel). The middle panels show the crossover between these two regimes. Figure 8 is a three-dimensional plot of $I(t)$ showing the crossover for $N = 30$.

In order to characterize the superradiant pulse in the intermediate regime, we compute its relative height A_I and the time t_I at which its maximum occurs. These quantities are defined as

$$A_I = \max_t[I(t)] - I(0) = I(t_I) - N\gamma_0. \quad (44)$$

Our results, displayed in Fig. 9, show that the height A_I of the pulse is maximal for $\Delta\gamma = 0$, decreases monotonically with $\Delta\gamma$, and vanishes for $\Delta\gamma \geqslant \Delta\gamma^*$, where the critical value $\Delta\gamma^*$ depends only on the number of atoms. The decrease as a function of $\Delta\gamma$ is more and more linear as N increases. We explain this behavior in the next section on the basis of a mean-field approximation. For sufficiently large N, the time t_I at which the maximum occurs increases as a function of $\Delta\gamma$ before dropping to zero at $\Delta\gamma = \Delta\gamma^*$. The critical value $\Delta\gamma^*$ increases as the number of atoms increases, as shown in Fig. 10, and tends to γ_0 for $N \to \infty$. This means that for a fixed value of $\Delta\gamma$, superradiance can always be observed for a sufficiently large number of atoms. Indeed, the derivative of the radiated energy rate (39) reads

$$\frac{dI(t)}{dt} = \sum_{J=J_{\min}}^{N/2} d_N^J \sum_{M=-J}^{J} \tilde{c}_J^M \rho_J^{M,M}(t), \quad (45)$$

with

$$\tilde{c}_J^M = 2(J + M)(J - M + 1)[(M - 1)\gamma - \Delta\gamma]\gamma$$
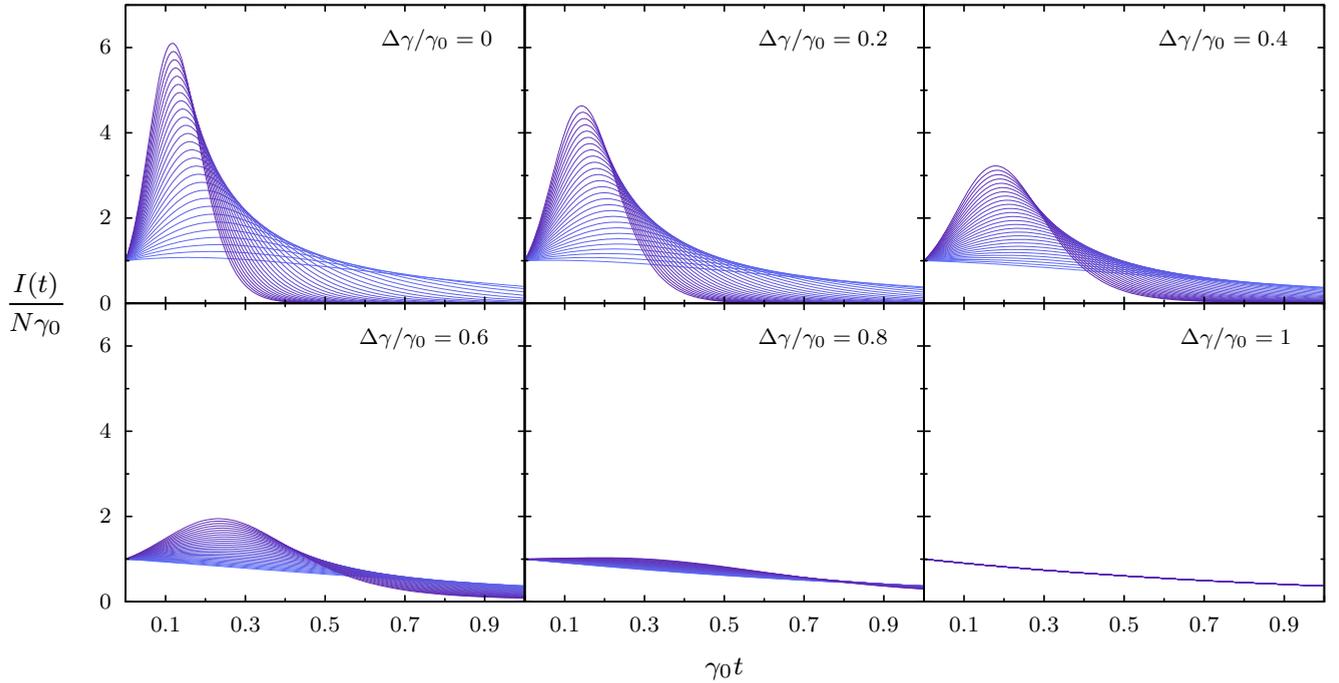$$- \left(M + \frac{N}{2}\right)\Delta\gamma^2. \quad (46)$$

FIG. 7. Radiated energy rate as a function of time for different values of $\Delta\gamma = \gamma_0 - \gamma$ (corresponding to the different panels) and different numbers of atoms ($N = 3, \ldots, 30$ from bottom to top on the left of each panel). The case $\Delta\gamma = 0$ (pure superradiance) is illustrated in the first panel, while the case $\Delta\gamma = \gamma_0$ corresponding to independent spontaneous emissions is illustrated in the last panel.

If the derivative of the radiated energy rate at initial time is strictly positive, a nonzero superradiant pulse height ($A_I > 0$) is always obtained. For an initial fully excited state, this sufficient condition in terms of the critical value $\Delta\gamma^*(N)$ reads

$$\Delta\gamma < \gamma_0\left(1 - \frac{1}{\sqrt{N-1}}\right) \equiv \Delta\gamma^*(N). \qquad (47)$$

As shown in Fig. 10, our numerical results are in excellent agreement with Eq. (47).
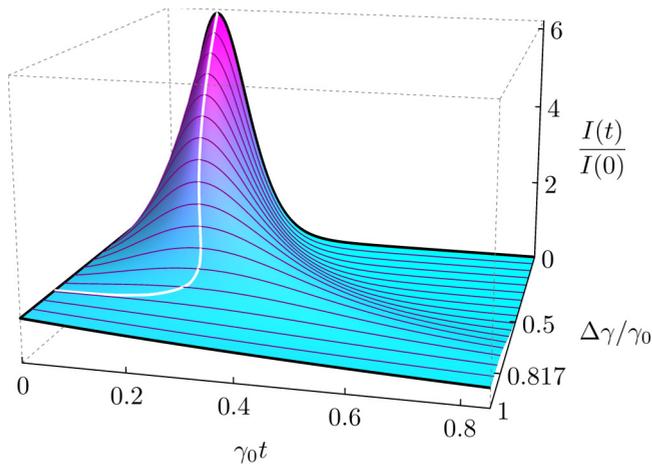

FIG. 8. Radiated energy rate as a function of time and $\Delta\gamma$ for $N = 30$ atoms. The superradiant pulse progressively disappears as $\Delta\gamma$ increases from 0 to $\Delta\gamma^* = 0.817\gamma_0$. For $\Delta\gamma = \gamma_0$, $I(t)$ decays exponentially at a rate γ_0. The white line indicates the location of the maximum of the pulse.

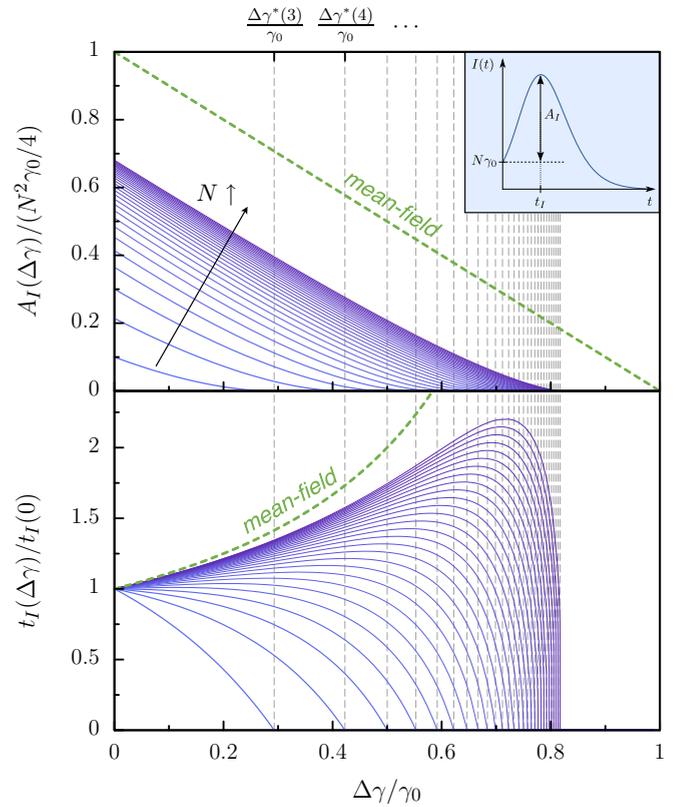FIG. 9. Shown on top is the height A_I of the superradiant pulse rescaled by $N^2\gamma_0/4$ as a function of $\Delta\gamma = \gamma_0 - \gamma$ for $N = 3, \ldots, 30$ (from left to right). The bottom shows the delay time $t_I(\Delta\gamma)$ after which the radiated intensity attains a maximum, rescaled by $t_I(0)$. The dashed green curves correspond to the mean-field results [Eqs. (60) and (62)].
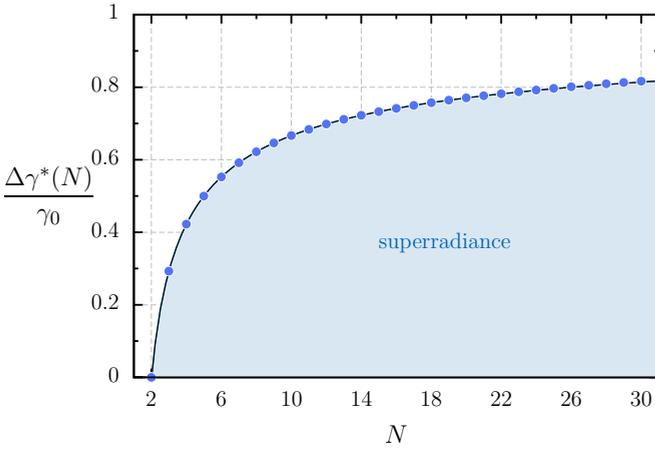
FIG. 10. Critical value $\Delta\gamma^*$ at which the superradiant pulse height A_I drops to zero and remains zero for $\Delta\gamma > \Delta\gamma^*$, plotted as a function of the number of atoms. The circles show the values extracted from numerical computations. The solid line shows the analytical prediction given by Eq. (47).

3. Mean-field approach

When the number of atoms is large, a mean-field approximation can be made [54,55] that assumes an internal state of the form

$$\rho(t) \approx \sigma(t) \otimes \cdots \otimes \sigma(t). \tag{48}$$

In the mean-field approximation, all atoms lie in the same quantum state $\sigma(t)$. The global state $\rho(t)$ is permutation invariant at any time t but not necessarily symmetric. However, when $\sigma(t)$ is a pure state, $\rho(t)$ is symmetric and has only components in the block of maximal angular momentum $J = N/2$. When $\Delta\gamma = 0$, the superradiant cascade takes place only in the block $J = N/2$ and $\sigma(t)$ is usually chosen pure [54]. When $\Delta\gamma \neq 0$, the ratio between the transition rates within the block $J = N/2$ and the neighboring block $J = N/2 - 1$ for the emission of the sth photon with $s \gg 1$ is much larger than 1, i.e.,

$$\frac{\Gamma^{(2)}_{N/2-s+1,N/2-s+1}}{\Gamma^{(3)}_{N/2-s+1,N/2-s+1}} \approx s\frac{\gamma}{\Delta\gamma} \gg 1. \tag{49}$$

Hence, during the main part of the radiative cascade (when s is large), the dynamics takes place essentially in the block $J = N/2$, so we also choose $\sigma(t)$ to be a pure state.

By inserting Eq. (48) into the master equation (3) and tracing over $N - 1$ atoms, we get the following nonlinear equation for $\sigma(t)$:

$$\frac{d\sigma(t)}{dt} = -\frac{i}{\hbar}\{V_H[\sigma(t)] + V_D[\sigma(t)],\sigma(t)\} + \mathcal{D}_{se}[\sigma(t)]. \tag{50}$$

In Eq. (50), V_H is the nonlinear Hartree potential (proportional to the dipole-dipole shift Δ_{dd})

$$V_H[\sigma(t)] = \hbar\Delta_{dd}(N-1)(\langle\sigma_+\rangle\sigma_- + \langle\sigma_-\rangle\sigma_+), \tag{51}$$

where $\langle\cdot\rangle = \text{Tr}[\cdot\,\sigma(t)]$, V_D is the nonlinear dissipative potential

$$V_D[\sigma(t)] = i\hbar\gamma\frac{N-1}{2}(\langle\sigma_+\rangle\sigma_- - \langle\sigma_-\rangle\sigma_+), \tag{52}$$

and $\mathcal{D}_{se}$ is the single-atom dissipator accounting for spontaneous emission

$$\mathcal{D}_{se}[\sigma(t)] = \gamma_0\big[\sigma_-\sigma(t)\sigma_+ - \tfrac{1}{2}\{\sigma_+\sigma_-,\sigma(t)\}\big]. \tag{53}$$

Equation (50) cannot be solved analytically because of the presence of the term (53). However, as N gets large, this one can be neglected in comparison to (51) and (52) provided $\gamma \neq 0$ and $N - 1$ can be replaced by N. Equation (50) can then be related for pure states $\sigma_\psi(t) = |\psi(t)\rangle\langle\psi(t)|$ to a nonlinear Schrödinger equation for $|\psi(t)\rangle$ of the form (in the interaction picture) [54,56,57]

$$\frac{d|\psi(t)\rangle}{dt} = -\frac{i}{\hbar}\{V_H[\sigma_\psi(t)] + V_D[\sigma_\psi(t)]\}|\psi(t)\rangle. \tag{54}$$

As in [54], we parametrize the state $|\psi(t)\rangle$ by

$$|\psi(t)\rangle = \sqrt{p(t)}e^{i\theta(t)}|e\rangle + \sqrt{1-p(t)}|g\rangle, \tag{55}$$

with $p(t) = |\langle e|\psi(t)\rangle|^2$ the mean number of atoms in the excited state. By inserting Eq. (55) into (54) we get

$$\frac{dp(t)}{dt} = -N\gamma p(t)[1 - p(t)], \tag{56a}$$

$$\frac{d\theta(t)}{dt} = -N\Delta_{dd}[1 - p(t)]. \tag{56b}$$

With the conditions $p(t_I) = 1/2$ and $\theta(0) = \theta_0$, the system of equations (56) has the unique solution

$$p(t) = \frac{1}{1 + e^{N\gamma(t-t_I)}}, \tag{57}$$

$$\theta(t) = \theta_0 + \frac{\Delta_{dd}}{\gamma}\ln[p(t)(1 + e^{-N\gamma t_I})], \tag{58}$$

where t_I corresponds to the time at which half the photons have been emitted and is identified with the delay time of superradiance [4]. The phase $\theta(t)$ depend on both the dipole-dipole shift Δ_{dd} and the decay rate γ, while the population $p(t)$ depends only on the rate γ. In other words, the dissipative dynamics is not affected by the dipole-dipole shift. The radiated energy rate in the mean-field approximation reads

$$I_{mf}(t) = -N\frac{dp(t)}{dt} = \frac{N^2\gamma}{4}\cosh^{-2}\left[\frac{N\gamma}{2}(t - t_I)\right] \tag{59}$$

and is of the same form as the pure superradiant pulse for colocated atoms [4,54], but with γ_0 replaced by γ and *a priori* a different delay time t_I. The quantum fluctuations of the atomic positions modify the value of γ as compared to γ_0, and thus the shape of the superradiant pulse, which is, however, always present except for $\gamma = 0$. The height $A_{I,mf}$ of the pulse (59), given by

$$A_{I,mf} = \frac{N^2\gamma}{4} = \frac{N^2\gamma_0}{4}\left(1 - \frac{\Delta\gamma}{\gamma_0}\right), \tag{60}$$

is always smaller than the height $N^2\gamma_0/4$ of the pure superradiant pulse since $\gamma \leqslant \gamma_0$. Equation (60) is compared with numerical simulations in Fig. 9 (green dashed curve, top

panel). As for the delay time t_I, it cannot be evaluated precisely in the mean-field approach. Nevertheless, an approximation can be obtained in the limit $N \to \infty$ and for $\gamma \neq 0$ by evaluating the sum of the typical times between each photon emission [4]. We find

$$t_I \sim \frac{\ln N}{N\gamma}, \tag{61}$$

which corresponds to the result of Gross and Haroche [4] but with γ_0 replaced by γ. The ratio between the delay time for $\Delta\gamma \neq 0$ and the one for $\Delta\gamma = 0$ (pure superradiance) is thus given by

$$\frac{t_I(\Delta\gamma)}{t_I(0)} = \frac{\gamma_0}{\gamma} = \frac{1}{1 - \Delta\gamma/\gamma_0}. \tag{62}$$

It is always larger than 1 and increases with $\Delta\gamma$, meaning that the larger $\Delta\gamma$ is, the longer it takes before the radiated energy rate attains a maximum. Equation (62) is compared with numerical simulations in Fig. 9 (green dashed curve, bottom panel).

B. Subradiance

Subradiant states are states for which the radiated energy rate decays slowly as compared to the one corresponding to independent spontaneous emission. Dark (or decoherence-free) states are a particular class of subradiant states for which the radiated energy rate (39) vanishes. According to Eq. (40), their only nonzero populations $\rho_J^{M,M}$ are those for which J and M are such that $c_J^M = 0$. When $\Delta\gamma = 0$, the condition $c_J^M = 0$ is satisfied for $M = -J$ [58]. As a consequence, all states $|J, -J\rangle$ (in number $\alpha_N^{J_{\min}}$; see, e.g., [59]) are dark states. When $\Delta\gamma > 0$, the only dark state is obtained for $J = M = N/2$ and corresponds to the ground state $|g, \ldots, g\rangle$.

In the following we study the time evolution of the state $|J_0, -J_0\rangle$ (with $J_0 \in \{J_{\min}, \ldots, N/2\}$) when $\Delta\gamma > 0$. The initial nonzero matrix element $\rho_{J_0}^{-J_0, -J_0}$ is only coupled to the matrix elements $\rho_J^{-J, -J}$ with higher angular momenta J, i.e., $J_0 \leqslant J \leqslant N/2$, as can be seen from Fig. 5. The system will thus gradually populate all states $|J, -J\rangle$ with $J > J_0$ before finally reaching the ground state $|N/2, -N/2\rangle$. The populations $\rho_J^{-J, -J}$ are obtained from Eq. (35), which simplifies to

$$\frac{d\rho_J^{-J, -J}(t)}{dt} = -\Delta\gamma \left[\left(\frac{N}{2} - J \right) \rho_J^{-J, -J}(t) \right.$$
$$\left. - \frac{d_N^{J-1}}{d_N^J} \left(\frac{N}{2} - J + 1 \right) \rho_{J-1}^{-J+1, -J+1}(t) \right] \tag{63}$$

and admits the solution

$$\rho_J^{-J, -J}(t) = \frac{\left(\frac{N}{2} - J_0 \right)! e^{-\Delta\gamma(N/2 - J_0)t}}{d_N^J \left(\frac{N}{2} - J \right)! (J - J_0)!} (e^{\Delta\gamma t} - 1)^{J - J_0}. \tag{64}$$

Inserting this expression into Eq. (39) for the radiated energy rate yields after some calculations

$$I(t) = \Delta\gamma \left(\frac{N}{2} - J_0 \right) e^{-\Delta\gamma t}. \tag{65}$$

Hence, $I(t)$ decreases exponentially regardless of the initial angular momentum J_0, except for the case $J_0 = N/2$ (ground state) for which $I(t) = 0$ at any time t. We also see that the states $|J_0, -J_0\rangle$ are subradiant, since the emission rate $\Delta\gamma$ is always smaller than γ_0, the single-atom spontaneous emission rate.

V. CONCLUSION

We have investigated superradiance and subradiance from indistinguishable atoms with quantized motional state based on the master equation derived in [43]. The indistinguishability of the atoms implies that for an initially factorized state between the external (center-of-mass) and internal degrees of freedom the motional state must be invariant under permutation of atoms. As a consequence, the whole dynamics is parametrized only by three real numbers, namely, the diagonal γ_0 and off-diagonal $\gamma \leqslant \gamma_0$ decay rates and a dipole-dipole shift Δ_{dd} that is identical for all atoms. All three parameters can be "quantum programmed" by appropriate choice of the motional state of the atoms. For $\gamma = \gamma_0$ standard superradiance results, whereas for $\gamma \to 0$ individual spontaneous emission of the atoms prevails. A continuous transition between these two extreme cases can be achieved. A superradiant enhancement of the emitted intensity is always observed for $\gamma > \gamma_0/\sqrt{N-1}$, where N is the number of atoms. All nontrivial dark states (i.e., states other than the ground state with strictly vanishing emission of radiation) are immediately lost as soon as $\gamma < \gamma_0$. This implies that for harmonically trapped atoms, exact decoherence free subspaces that protect against spontaneous emission through destructive interference of individual spontaneous emission amplitudes exist only in the limit of classically localized atoms, i.e., atoms in infinitely steep traps. Finally, we showed that the states that are dark when $\gamma = \gamma_0$ are only subradiant when $\gamma < \gamma_0$.

APPENDIX A: SYMMETRY OF THE DENSITY MATRIX UNDER PERMUTATION OF INDISTINGUISHABLE ATOMS

In this appendix we give general properties under permutation of atoms of the (reduced) density matrices describing the states of indistinguishable atoms. Consider a set of N indistinguishable atoms (bosons or fermions) with internal and external degrees of freedom. We define the orthonormal basis vectors as $|\boldsymbol{\nu}\rangle|\boldsymbol{\phi}\rangle \equiv |\nu_1, \ldots, \nu_N\rangle|\phi_1, \ldots, \phi_N\rangle$, where $|\nu_j\rangle$ ($|\phi_j\rangle$) are the internal (external) orthonormal basis states of the particle j. The permutation operator P_π corresponding to the permutation π is defined through exchange of the particle labels in the basis states, i.e.,

$$P_\pi |\boldsymbol{\nu}\rangle|\boldsymbol{\phi}\rangle = |\nu_{\pi_1}, \ldots, \nu_{\pi_N}\rangle|\phi_{\pi_1}, \ldots, \phi_{\pi_N}\rangle \equiv |\boldsymbol{\nu}_\pi\rangle|\boldsymbol{\phi}_\pi\rangle. \tag{A1}$$

We have $P_\pi = P_\pi^{\mathrm{in}} \otimes P_\pi^{\mathrm{ex}}$, where P_π^{in} and P_π^{ex} are such that $P_\pi^{\mathrm{in}}|\boldsymbol{\nu}\rangle = |\boldsymbol{\nu}_\pi\rangle$ and $P_\pi^{\mathrm{ex}}|\boldsymbol{\phi}\rangle = |\boldsymbol{\phi}_\pi\rangle$.

An arbitrary pure state $|\psi\rangle$ of the full system can be written as

$$|\psi\rangle = \sum_{\boldsymbol{\nu\phi}} \alpha_{\boldsymbol{\nu\phi}} |\boldsymbol{\nu}\rangle |\boldsymbol{\phi}\rangle \qquad (A2)$$

and must be invariant under permutations up to a global phase, i.e., $P_\pi |\psi\rangle = (\pm)^{p_\pi} |\psi\rangle$, where p_π is the parity of the permutation (even or odd) and $(\pm)^{p_\pi}$ the phase factor picked up accordingly for bosons (+) or fermions (−). Then we have the following:

Lemma 1. An arbitrary mixed state ρ of indistinguishable bosons or fermions (density operator on the full Hilbert space) satisfies

$$P_\pi \rho P_{\pi'}^\dagger = (\pm)^{p_\pi + p_{\pi'}} \rho \quad \forall \pi, \pi'. \qquad (A3)$$

Proof. The mixed state of a system of indistinguishable bosons (fermions) must be a mixture of pure states that have all the full permutation symmetry (antisymmetry), i.e.,

$$\rho = \sum_i p_i |\psi^{(i)}\rangle \langle \psi^{(i)}|, \qquad (A4)$$

where p_i are probabilities and $P_\pi |\psi^{(i)}\rangle = (\pm)^{p_\pi} |\psi^{(i)}\rangle$ for all i. Applying P_π from the left and $P_{\pi'}^\dagger$ from the right immediately yields the claim. ∎

Consider now the reduced density matrix corresponding to the internal degrees of freedom only. Inserting the decomposition (A2) for each state $|\psi^{(i)}\rangle$ in the convex sum (A4), we obtain

$$\rho^{\text{in}} \equiv \text{Tr}_{\text{ex}}\rho = \sum_{\boldsymbol{\phi}} \langle \boldsymbol{\phi}|\rho|\boldsymbol{\phi}\rangle = \sum_i p_i \sum_{\boldsymbol{\phi},\boldsymbol{\nu},\boldsymbol{\mu}} \alpha_{\boldsymbol{\nu\phi}}^{(i)} \alpha_{\boldsymbol{\mu\phi}}^{(i)*} |\boldsymbol{\nu}\rangle \langle \boldsymbol{\mu}|. \qquad (A5)$$

Similarly, the reduced density matrix corresponding to the external degrees of freedom reads

$$\rho^{\text{ex}} \equiv \text{Tr}_{\text{in}}\rho = \sum_{\boldsymbol{\nu}} \langle \boldsymbol{\nu}|\rho|\boldsymbol{\nu}\rangle = \sum_i p_i \sum_{\boldsymbol{\nu},\boldsymbol{\phi},\boldsymbol{\psi}} \alpha_{\boldsymbol{\nu\phi}}^{(i)} \alpha_{\boldsymbol{\nu\psi}}^{(i)*} |\boldsymbol{\phi}\rangle \langle \boldsymbol{\psi}|. \qquad (A6)$$

Then we have the following.

Lemma 2. The arbitrary reduced density matrices ρ^{in} and ρ^{ex} of indistinguishable atoms (bosons or fermions) satisfy

$$\begin{aligned} P_\pi^{\text{in}} \rho^{\text{in}} P_\pi^{\text{in}\dagger} &= \rho^{\text{in}} \, \forall \pi, \\ P_\pi^{\text{ex}} \rho^{\text{ex}} P_\pi^{\text{ex}\dagger} &= \rho^{\text{ex}} \, \forall \pi. \end{aligned} \qquad (A7)$$

Proof. We present here the proof for ρ^{in}. The symmetry of the full state implies the symmetry of the coefficients $\alpha_{\boldsymbol{\nu\phi}}^{(i)}$,

$$P_\pi |\psi^{(i)}\rangle = \sum_{\boldsymbol{\nu\phi}} \alpha_{\boldsymbol{\nu\phi}}^{(i)} |\boldsymbol{\nu}_\pi\rangle |\boldsymbol{\phi}_\pi\rangle \qquad (A8)$$

$$= \sum_{\boldsymbol{\nu\phi}} \alpha_{\boldsymbol{\nu}_{\pi^{-1}}\boldsymbol{\phi}_{\pi^{-1}}}^{(i)} |\boldsymbol{\nu}\rangle |\boldsymbol{\phi}\rangle = (\pm)^{p_\pi} |\psi^{(i)}\rangle, \quad (A9)$$

and projecting onto the basis states gives

$$(\pm)^{p_\pi} \alpha_{\boldsymbol{\nu\phi}}^{(i)} = \alpha_{\boldsymbol{\nu}_{\pi^{-1}}\boldsymbol{\phi}_{\pi^{-1}}}^{(i)}. \qquad (A10)$$

As a consequence,

$$\begin{aligned} P_\pi^{\text{in}} \rho^{\text{in}} P_\pi^{\text{in}\dagger} &= \sum_{i,\boldsymbol{\phi},\boldsymbol{\nu},\boldsymbol{\mu}} p_i \alpha_{\boldsymbol{\nu\phi}}^{(i)} \alpha_{\boldsymbol{\mu\phi}}^{(i)*} |\boldsymbol{\nu}_\pi\rangle \langle \boldsymbol{\mu}_\pi| \\ &= \sum_{i,\boldsymbol{\phi},\boldsymbol{\nu},\boldsymbol{\mu}} p_i \alpha_{\boldsymbol{\nu}_{\pi^{-1}}\boldsymbol{\phi}}^{(i)} \alpha_{\boldsymbol{\mu}_{\pi^{-1}}\boldsymbol{\phi}}^{(i)*} |\boldsymbol{\nu}\rangle \langle \boldsymbol{\mu}| \\ &= \sum_{i,\boldsymbol{\phi},\boldsymbol{\nu},\boldsymbol{\mu}} p_i \alpha_{\boldsymbol{\nu}_{\pi^{-1}}\boldsymbol{\phi}_{\pi^{-1}}}^{(i)} \alpha_{\boldsymbol{\mu}_{\pi^{-1}}\boldsymbol{\phi}_{\pi^{-1}}}^{(i)*} |\boldsymbol{\nu}\rangle \langle \boldsymbol{\mu}| = \rho^{\text{in}}, \end{aligned}$$

where in the penultimate step permutation π was absorbed in the sum over all $\boldsymbol{\phi}$ and the last step follows from Eqs. (A10) and (A5). ∎

Note that in general for the reduced density matrix ρ^{in} the statement corresponding to Eq. (A3) does not hold, i.e., $P_\pi \rho^{\text{in}} P_{\pi'}^\dagger \neq \rho^{\text{in}}$ for $\pi \neq \pi'$: Going through the last proof again with the second π replaced by π', one realizes that in at least one of the coefficients $\alpha_{\boldsymbol{\nu}_{\pi^{-1}}\boldsymbol{\phi}}^{(i)}$ or $\alpha_{\boldsymbol{\mu}_{\pi'^{-1}}\boldsymbol{\phi}}^{(i)*}$, $\boldsymbol{\phi}$ cannot be replaced by $\boldsymbol{\phi}_{\pi^{-1}}$ or $\boldsymbol{\phi}_{\pi'^{-1}}$ if $\pi \neq \pi'$, and in general $\alpha_{\boldsymbol{\nu\phi}} \neq \alpha_{\boldsymbol{\nu}_{\pi^{-1}}\boldsymbol{\phi}_{\pi'^{-1}}}$ even for bosons.

APPENDIX B: GENERAL EXPRESSIONS OF DECAY RATES AND DIPOLE-DIPOLE SHIFTS

In this appendix we show that all off-diagonal ($i \neq j$) decay rates γ_{ij} and all dipole-dipole shifts Δ_{ij} are equal for any pair of indistinguishable atoms i and j in arbitrary permutation invariant motional states. Then we give their general expressions for arbitrary symmetric or antisymmetric motional states.

As shown in [43], the diagonal decay rates are equal to the single-atom spontaneous emission rate γ_0 for any motional state, while the off-diagonal decay rates and dipole-dipole shifts are given, respectively, by

$$\gamma_{ij} = \int_{\mathbb{R}^3} \gamma^{\text{cl}}(\mathbf{r}) \mathcal{F}_{\mathbf{r}}^{-1}[\mathcal{C}_{ij}^{\text{ex}}(\mathbf{k})] d\mathbf{r}, \qquad (B1)$$

$$\Delta_{ij} = \int_{\mathbb{R}^3} \Delta^{\text{cl}}(\mathbf{r}) \mathcal{F}_{\mathbf{r}}^{-1}[\mathcal{C}_{ij}^{\text{ex}}(\mathbf{k})] d\mathbf{r}, \qquad (B2)$$

with $\mathcal{F}_{\mathbf{r}}^{-1}[\mathcal{C}_{ij}^{\text{ex}}(\mathbf{k})]$ the inverse Fourier transform of the motional correlation function [60]

$$\mathcal{C}_{ij}^{\text{ex}}(\mathbf{k}) = \text{Tr}_{\text{ex}}[e^{i\mathbf{k}\cdot\hat{\mathbf{r}}_{ij}} \rho_A^{\text{ex}}], \qquad (B3)$$

where $\hat{\mathbf{r}}_{ij} = \hat{\mathbf{r}}_i - \hat{\mathbf{r}}_j$ is the difference between the position operators of atoms i and j. In Eqs. (B1) and (B2), $\gamma^{\text{cl}}(\mathbf{r})$ and $\Delta^{\text{cl}}(\mathbf{r})$ are the classical expressions of the decay rates and dipole-dipole shifts, respectively, for a pair of atoms connected by $\mathbf{r}$ and a radiation of wave number k_0 [61–63],

$$\gamma^{\text{cl}}(\mathbf{r}) = \frac{3\gamma_0}{2}\left[p\frac{\sin(k_0 r)}{k_0 r} + q\left(\frac{\cos(k_0 r)}{(k_0 r)^2} - \frac{\sin(k_0 r)}{(k_0 r)^3}\right)\right] \qquad (B4)$$

and

$$\Delta^{\text{cl}}(\mathbf{r}) = \frac{3\gamma_0}{4}\left[-p\frac{\cos(k_0 r)}{k_0 r} + q\left(\frac{\sin(k_0 r)}{(k_0 r)^2} + \frac{\cos(k_0 r)}{(k_0 r)^3}\right)\right], \qquad (B5)$$

with p and q angular factors given by

$$p = \begin{cases} \sin^2 \alpha & \text{for a } \pi \text{ transition} \\ \frac{1}{2}(1 + \cos^2 \alpha) & \text{for a } \sigma^{\pm} \text{ transition} \end{cases} \quad \text{(B6)}$$

and

$$q = \begin{cases} 1 - 3\cos^2 \alpha & \text{for a } \pi \text{ transition} \\ \frac{1}{2}(3\cos^2 \alpha - 1) & \text{for a } \sigma^{\pm} \text{ transition,} \end{cases} \quad \text{(B7)}$$

where $\alpha = \arccos(\mathbf{e}_r \cdot \mathbf{e}_z)$ is the angle between the quantization axis and $\mathbf{r}$.

Indistinguishability of atoms implies that their motional state is invariant under permutation [see Appendix A], i.e.,

$$P_{\pi}^{\text{ex}} \rho_A^{\text{ex}} P_{\pi}^{\text{ex}\dagger} = \rho_A^{\text{ex}} \; \forall \pi. \quad \text{(B8)}$$

Upon using the latter equation, the motional correlation function (B3) is found to satisfy

$$\begin{aligned} \mathcal{C}_{ij}^{\text{ex}}(\mathbf{k}) &= \text{Tr}_{\text{ex}}\left[e^{i\mathbf{k}\cdot\hat{\mathbf{r}}_{ij}} P_{\pi}^{\text{ex}} \rho_A^{\text{ex}} P_{\pi}^{\text{ex}\dagger} \right] \\ &= \text{Tr}_{\text{ex}}\left[P_{\pi}^{\text{ex}\dagger} e^{i\mathbf{k}\cdot\hat{\mathbf{r}}_{ij}} P_{\pi}^{\text{ex}} \rho_A^{\text{ex}} \right] \\ &= \text{Tr}_{\text{ex}}\left[e^{i\mathbf{k}\cdot\hat{\mathbf{r}}_{\pi(i)\pi(j)}} \rho_A^{\text{ex}} \right] = \mathcal{C}_{\pi(i)\pi(j)}^{\text{ex}}(\mathbf{k}). \end{aligned} \quad \text{(B9)}$$

The equality of $\mathcal{C}_{ij}^{\text{ex}}(\mathbf{k})$ for any pair of atoms [Eq. (B9)] implies the equality of the decay rates (B1) [or the dipole-dipole shifts (B2)] for any pair of atoms.

Consider now an arbitrary symmetric or antisymmetric motional state of the form

$$\rho_A^{\text{ex},\pm} = \sum_{m=1}^{M} p_m \left| \Phi_A^{(m),\pm} \right\rangle \left\langle \Phi_A^{(m),\pm} \right|, \quad \text{(B10)}$$

where p_m are the weights of the statistical mixture ($p_m \geqslant 0$ and $\sum_m p_m = 1$) and $|\Phi_A^{(m),\pm}\rangle$ ($m = 1, \ldots, M$) are symmetric (+) or antisymmetric (−) N-atom motional pure states. Any state $|\Phi_A^{(m),\pm}\rangle$ can be written as

$$\left| \Phi_A^{(m),\pm} \right\rangle = \sqrt{\frac{n_{\phi_1^{(m)}}! \cdots n_{\phi_N^{(m)}}!}{N!}} \sum_{\pi} (\pm 1)^{p_{\pi}} \left| \phi_{\pi(1)}^{(m)} \cdots \phi_{\pi(N)}^{(m)} \right\rangle, \quad \text{(B11)}$$

where $|\phi_j^{(m)}\rangle$ ($j = 1, \ldots, N$) are normalized (but not necessarily orthogonal) single-atom motional states, $n_{\phi_j^{(m)}}$ is the number of atoms occupying the state $|\phi_j^{(m)}\rangle$, and the sum runs over all permutations π of the atoms.

The off-diagonal decay rates and the dipole-dipole shifts for the motional state (B10) can be expressed in terms of exchange integrals as [43]

$$\begin{aligned} \gamma_{ij} = \sum_{m=1}^{M} p_m \sum_{\pi,\pi'} \lambda_{ij,\pi\pi'}^{(m),\pm} \iint_{\mathbb{R}^3 \times \mathbb{R}^3} \gamma^{\text{cl}}(\mathbf{r} - \mathbf{r}') \phi_{\pi(i)}^{(m)}(\mathbf{r}) \\ \times \phi_{\pi'(i)}^{(m)*}(\mathbf{r}) \phi_{\pi(j)}^{(m)}(\mathbf{r}') \phi_{\pi'(j)}^{(m)*}(\mathbf{r}') d\mathbf{r} \, d\mathbf{r}', \end{aligned} \quad \text{(B12)}$$

$$\begin{aligned} \Delta_{ij} = \sum_{m=1}^{M} p_m \sum_{\pi,\pi'} \lambda_{ij,\pi\pi'}^{(m),\pm} \iint_{\mathbb{R}^3 \times \mathbb{R}^3} \Delta^{\text{cl}}(\mathbf{r} - \mathbf{r}') \phi_{\pi(i)}^{(m)}(\mathbf{r}) \\ \times \phi_{\pi'(i)}^{(m)*}(\mathbf{r}) \phi_{\pi(j)}^{(m)}(\mathbf{r}') \phi_{\pi'(j)}^{(m)*}(\mathbf{r}') d\mathbf{r} \, d\mathbf{r}', \end{aligned} \quad \text{(B13)}$$

with $\phi_j^{(m)}(\mathbf{r}) = \langle \mathbf{r} | \phi_j^{(m)} \rangle$ the single-atom motional states in the position representation, and

$$\lambda_{ij,\pi\pi'}^{(m),\pm} = \frac{(\pm 1)^{p_\pi + p_{\pi'}} \prod_{\substack{n=1 \\ n \neq i,j}}^{N} \left\langle \phi_{\pi'(n)}^{(m)} \middle| \phi_{\pi(n)}^{(m)} \right\rangle}{\sum_{\tilde{\pi}, \tilde{\pi}'} (\pm 1)^{p_{\tilde{\pi}} + p_{\tilde{\pi}'}} \prod_{n=1}^{N} \left\langle \phi_{\tilde{\pi}'(n)}^{(m)} \middle| \phi_{\tilde{\pi}(n)}^{(m)} \right\rangle}. \quad \text{(B14)}$$

The cooperative decay rates and dipole-dipole shifts (B12) and (B13) depend on their classical expressions (B4) and (B5), which oscillate and decrease as a function of the interatomic distance on a length scale of the order of the wavelength of the emitted radiation. In addition, they depend on the single-atom wave packets and can vary as a function of their extensions and overlaps. The indistinguishability of atoms is reflected by the summations over all permutations of the atoms, which implies the equality of all off-diagonal decay rates γ_{ij} and all dipole-dipole shifts Δ_{ij}. Note that when all atoms occupy the same motional state ρ_1 with spatial density $\rho_1(\mathbf{r}) = \langle \mathbf{r} | \rho_1 | \mathbf{r} \rangle$, the global motional state $\rho_A^{\text{ex}} = \rho_1^{\otimes N}$ is symmetric and separable and the decay rates (B12) and dipole-dipole shifts (B13) merely read

$$\gamma_{ij} = \iint_{\mathbb{R}^3 \times \mathbb{R}^3} \gamma^{\text{cl}}(\mathbf{r} - \mathbf{r}') \rho_1(\mathbf{r}) \rho_1(\mathbf{r}') d\mathbf{r} \, d\mathbf{r}', \quad \text{(B15)}$$

$$\Delta_{ij} = \iint_{\mathbb{R}^3 \times \mathbb{R}^3} \Delta^{\text{cl}}(\mathbf{r} - \mathbf{r}') \rho_1(\mathbf{r}) \rho_1(\mathbf{r}') d\mathbf{r} \, d\mathbf{r}'. \quad \text{(B16)}$$

APPENDIX C: GENERAL SOLUTION FOR TWO ATOMS

In this appendix we give the most general solution of the master equation (3) for $N = 2$ atoms. In this case, $J = 0, 1$ and the decomposition (20) of the internal Hilbert space of the atomic system reads

$$\mathcal{H} = \mathbb{C}^2 \otimes \mathbb{C}^2 \simeq (\mathcal{H}_0 \otimes \mathcal{K}_0) \oplus (\mathcal{H}_1 \otimes \mathcal{K}_1), \quad \text{(C1)}$$

where the dimensions of $\mathcal{K}_0$ and $\mathcal{K}_1$ are $d_0 = d_1 = 1$. The value $J = 1$ defines the triplet states $\{|1,1\rangle, |1,0\rangle, |1,-1\rangle\}$, which are all symmetric, while the value $J = 0$ corresponds to the singlet state $|0,0\rangle$, which is antisymmetric. In the standard basis $\{|e,e\rangle, |e,g\rangle, |g,e\rangle, |g,g\rangle\}$, they read

$$\begin{aligned} |1,1\rangle &= |e,e\rangle, \\ |1,0\rangle &= \frac{|e,g\rangle + |g,e\rangle}{\sqrt{2}}, \\ |1,-1\rangle &= |g,g\rangle, \quad |0,0\rangle = \frac{|e,g\rangle - |g,e\rangle}{\sqrt{2}}. \end{aligned} \quad \text{(C2)}$$

The solutions of (35) for the density matrix elements $\rho_J^{M,M'}(t)$ in terms of γ, $\Delta\gamma$, and Δ_{dd} are in this case given by

$$\rho_1^{1,1}(t) = \rho_1^{1,1}(0)e^{-2(\gamma+\Delta\gamma)t}, \quad \rho_1^{0,0}(t) = \rho_1^{0,0}(0)e^{-(2\gamma+\Delta\gamma)t} + \frac{2\gamma+\Delta\gamma}{\Delta\gamma}\rho_1^{1,1}(t)(e^{\Delta\gamma t}-1),$$

$$\rho_1^{-1,-1}(t) = 1 - \rho_1^{1,1}(t) - \rho_1^{0,0}(t) - \rho_0^{0,0}(t), \quad \rho_0^{0,0}(t) = \rho_0^{0,0}(0)e^{-\Delta\gamma t} + \frac{\Delta\gamma}{2\gamma+\Delta\gamma}\rho_1^{1,1}(t)(e^{(2\gamma+\Delta\gamma)t}-1),$$

$$\rho_1^{1,0}(t) = \rho_1^{1,0}(0)e^{-(4\gamma+3\Delta\gamma+2i\Delta_{dd})t/2}, \quad \rho_1^{1,-1}(t) = \rho_1^{1,-1}(0)e^{-(\gamma+\Delta\gamma)t},$$

$$\rho_1^{0,-1}(t) = \rho_1^{0,-1}(0)e^{-(2\gamma+\Delta\gamma-2i\Delta_{dd})t/2} + \rho_1^{1,0}(t)\frac{2\gamma+\Delta\gamma}{\gamma+\Delta\gamma+2i\Delta_{dd}}(e^{(\gamma+\Delta\gamma+2i\Delta_{dd})t}-1). \tag{C3}$$

[1] R. H. Dicke, Phys. Rev. **93**, 99 (1954).
[2] R. Friedberg, S. R. Hartmann, and J. T. Manassah, Phys. Lett. A **40**, 365 (1972).
[3] F. Friedberg and S. R. Hartmann, Phys. Rev. A **10**, 1728 (1974).
[4] M. Gross and S. Haroche, Phys. Rep. **93**, 301 (1982).
[5] B. Coffey and R. Friedberg, Phys. Rev. A **17**, 1033 (1978).
[6] H. S. Freedhoff, J. Phys. B **19**, 3035 (1986).
[7] H. S. Freedhoff, J. Phys. B **20**, 285 (1987).
[8] T. Richter, J. Phys. B **23**, 4415 (1990).
[9] W. Feng, Y. Li, and S.-Y. Zhu, Phys. Rev. A **88**, 033856 (2013).
[10] M. O. Scully, E. S. Fry, C. H. Ooi, and K. Wódkiewicz, Phys. Rev. Lett. **96**, 010501 (2006).
[11] M. O. Scully and A. A. Svidzinsky, Science **325**, 1510 (2009).
[12] R. A. de Oliveira, M. S. Mendes, W. S. Martins, P. L. Saldanha, J. W. R. Tabosa, and D. Felinto, Phys. Rev. A **90**, 023848 (2014).
[13] X. Kong and A. Pálffy, arXiv:1606.02988.
[14] T. Bienaimé, N. Piovella, and R. Kaiser, Phys. Rev. Lett. **108**, 123602 (2012).
[15] W. Guerin, M. O. Araùjo, and R. Kaiser, Phys. Rev. Lett. **116**, 083601 (2016).
[16] R. Röhlsberger, K. Schlage, B. Sahoo, S. Couet, and R. Rüffer, Science **328**, 1248 (2010).
[17] Z. Meir, O. Schwartz, E. Shahmoon, D. Oron, and R. Ozeri, Phys. Rev. Lett. **113**, 193002 (2014).
[18] E. Akkermans, A. Gero, and R. Kaiser, Phys. Rev. Lett. **101**, 103602 (2008).
[19] C. E. Máximo, N. Piovella, P. W. Courteille, R. Kaiser, and R. Bachelard, Phys. Rev. A **92**, 062702 (2015).
[20] R. Wiegner, J. von Zanthier, and G. S. Agarwal, Phys. Rev. A **84**, 023805 (2011).
[21] R. Wiegner, S. Oppel, D. Bhatti, J. von Zanthier, and G. S. Agarwal, Phys. Rev. A **92**, 033832 (2015).
[22] M. Wilkens and P. Meystre, Opt. Commun. **94**, 66 (1992).
[23] J. Javanainen, Phys. Rev. Lett. **72**, 2375 (1994).
[24] L. You, M. Lewenstein, and J. Cooper, Phys. Rev. A **50**, R3565(R) (1994).
[25] P. R. Berman, Phys. Rev. A **55**, 4466 (1997).
[26] D. Braun and J. Martin, Phys. Rev. A **77**, 032102 (2008).
[27] Q. Li, D. Z. Xu, C. Y. Cai, and C. P. Sun, Sci. Rep. **3**, 3144 (2013).
[28] J. Dalibard and C. Cohen-Tannoudji, J. Opt. Soc. Am. B **2**, 1707 (1985).
[29] V. G. Minogin and V. S. Letokhov, *Laser Light Pressure on Atoms* (CRC, Boca Raton, 1987).

[30] C. N. Cohen-Tannoudji, Rev. Mod. Phys. **70**, 707 (1998).
[31] C. E. Wieman, D. E. Pritchard, and D. J. Wineland, Rev. Mod. Phys. **71**, S253 (1999).
[32] P. Domokos and H. Ritsch, J. Opt. Soc. Am. B **20**, 1098 (2003).
[33] J. Schachenmayer, L. Pollet, M. Troyer, and A. J. Daley, Phys. Rev. A **89**, 011601 (2014).
[34] S. Sarkar, S. Langer, J. Schachenmayer, and A. J. Daley, Phys. Rev. A **90**, 023618 (2014).
[35] B. Zhu, J. Cooper, J. Ye, and A. M. Rey, Phys. Rev. A **94**, 023612 (2016).
[36] G. Labeyrie, D. Delande, R. Kaiser, and C. Miniatura, Phys. Rev. Lett. **97**, 013004 (2006).
[37] J. Pellegrino, R. Bourgain, S. Jennewein, Y. R. P. Sortais, A. Browaeys, S. D. Jenkins, and J. Ruostekoski, Phys. Rev. Lett. **113**, 133602 (2014).
[38] S. D. Jenkins, J. Ruostekoski, J. Javanainen, R. Bourgain, S. Jennewein, Y. R. P. Sortais, and A. Browaeys, Phys. Rev. Lett. **116**, 183601 (2016).
[39] S. D. Jenkins, J. Ruostekovski, J. Javanainen, S. Jennewein, R. Bourgain, J. Pellegrino, Y. R. P. Sortais, and A. Browaeys, Phys. Rev. A **94**, 023842 (2016).
[40] S. L. Bromley, B. Zhu, M. Bishof, X. Zhang, T. Bothwell, J. Schachenmayer, T. L. Nicholson, R. Kaiser, S. F. Yelin, M. D. Lukin, A. M. Rey, and J. Ye, Nat. Commun. **7**, 11039 (2016).
[41] M. Xu, S. B. Jäger, S. Schütz, J. Cooper, G. M. Morigi, and M. J. Holland, Phys. Rev. Lett. **116**, 153002 (2016).
[42] S. Inouye, A. P. Chikkatur, D. M. Stamper-Kurn, J. Stenger, D. E. Pritchard, and W. Ketterle, Science **285**, 571 (1999).
[43] F. Damanet, D. Braun, and J. Martin, Phys. Rev. A **93**, 022124 (2016).
[44] B. A. Chase and J. M. Geremia, Phys. Rev. A **78**, 052101 (2008).
[45] B. Q. Baragiola, B. A. Chase, and J. M. Geremia, Phys. Rev. A **81**, 032104 (2010).
[46] C. J. Pethick and H. Smith, *Bose-Einstein Condensation in Dilute Gases*, 2nd ed. (Cambridge University Press, Cambridge, 2008).
[47] L. D. Landau, E. M. Lifshitz, and L. Pitaevskii, *Statistical Physics*, 3rd ed. (Pergamon, Oxford, 1980), Vol. 5.
[48] L. Novo, T. Moroder, and O. Gühne, Phys. Rev. A **88**, 012305 (2013).
[49] G. M. D'Ariano, C. Macchiavello, and P. Perinotti, Phys. Rev. Lett. **95**, 060503 (2005).
[50] F. Buscemi, G. M. D'Ariano, C. Macchiavello, and P. Perinotti, Phys. Rev. A **74**, 042309 (2006).

[51] D. Bacon, I. L. Chuang, and A. W. Harrow, Phys. Rev. Lett. **97**, 170502 (2006).

[52] L. Arnaud, Phys. Rev. A **93**, 012320 (2016).

[53] M. Christandl, The structure of bipartite quantum states, Ph.D. thesis, University of Cambridge, 2006.

[54] H.-P. Breuer and F. Petruccione, *The Theory of Open Quantum Systems* (Oxford University Press, Oxford, 2006).

[55] H. Spohn, Rev. Mod. Phys. **52**, 569 (1980).

[56] L. Mandel and E. Wolf, *Optical Coherence and Quantum Optics* (Cambridge University Press, Cambridge, 1995).

[57] G. A. Prataviera and S. S. Mizrahi, Rev. Bras. Ensino Fís. **36**, 4303 (2014).

[58] R. I. Karasik, K.-P. Marzlin, B. C. Sanders, and K. B. Whaley, Phys. Rev. A **76**, 012331 (2007); **77**, 052301 (2008).

[59] D. Braun, *Dissipative Quantum Chaos and Decoherence*, Springer Tracts in Modern Physics Vol. 172 (Springer, Berlin, 2001).

[60] In this work, we use for the Fourier transform $\mathcal{F}_{\mathbf{k}}[\cdot]$ and its inverse $\mathcal{F}_{\mathbf{r}}^{-1}[\cdot]$ the convention $\mathcal{F}_{\mathbf{k}}[f] = \int_{\mathbb{R}^3} e^{-i\mathbf{k}\cdot\mathbf{r}} f(\mathbf{r})d\mathbf{r}$ and $\mathcal{F}_{\mathbf{r}}^{-1}[g] = \int_{\mathbb{R}^3} e^{i\mathbf{k}\cdot\mathbf{r}} g(\mathbf{k})\frac{d\mathbf{k}}{(2\pi)^3}$, respectively.

[61] M. J. Stephen, J. Chem. Phys. **40**, 669 (1964).

[62] R. H. Lehmberg, Phys. Rev. A **2**, 889 (1970).

[63] G. S. Agarwal, *Quantum Statistical Theories of Spontaneous Emission and Their Relation to Other Approaches*, Springer Tracts in Modern Physics Vol. 70 (Springer, Berlin, 1974), p. 1.